GEOARCHAEOLOGICAL X-RAY FLUORESCENCE SPECTROMETRY LABORATORY
8100 Wyoming Blvd., Ste M4-158 Albuquerque, NM 87113
USA

# SOURCE PROVENANCE OF OBSIDIAN ARTIFACTS FROM FIVE SITES IN SOUTHWEST UTAH

Obsidian at the Wild Horse Canyon source, Mineral Mountains, Utah. Photo courtesy of Joe Moore. Note the mahogany (red) colored nodules debitage of which is present in this assemblage

by

M. Steven Shackley, Ph.D., Director
Geoarchaeological XRF Laboratory
Albuquerque, New Mexico

Report Prepared for

Envirosystems
Flagstaff, Arizona

21 June 2021

## INTRODUCTION

The analysis here of 63 obsidian artifacts (three are not obsidian) from five sites in southwestern Utah, indicates a source provenance assemblage with artifacts mainly produced from two sources in southwestern Utah, Modena in Iron County and Wild Horse Canyon in Beaver County, and the Kane Springs source in Lincoln County, Nevada (Haarklau et al. 2005; see cover image,Tables 1 and 2, and Figures 1 and 2). One small piece of debitage was produced from the Obsidian Cliff source in the Yellowstone Plateau of northwestern Wyoming (source data at laboratory). Obsidian Cliff obsidian does occur in early contexts throughout the West and into the Middle West (Beck and Jones 2011; Davis et al. 1995; Scheiber and Finley 2011; Shackley 2014, 2017). See source discussion below.

## LABORATORY SAMPLING, ANALYSIS AND INSTRUMENTATION

All archaeological samples are analyzed whole. The results presented here are quantitative in that they are derived from "filtered" intensity values ratioed to the appropriate x-ray continuum regions through a least squares fitting formula rather than plotting the proportions of the net intensities in a ternary system (McCarthy and Schamber 1981; Schamber 1977). Or more essentially, these data through the analysis of international rock standards, allow for inter-instrument comparison with a predictable degree of certainty (Hampel 1984; Shackley 2011).

All analyses for this study were conducted on a ThermoScientific *Quant'X* EDXRF spectrometer, located at the Geoarchaeological XRF Laboratory, Albuquerque, New Mexico. It is equipped with a thermoelectrically Peltier cooled solid-state Si(Li) X-ray detector, with a 50 kV, 50 W, ultra-high-flux end window bremsstrahlung, Rh target X-ray tube and a 76 µm (3 mil) beryllium (Be) window (air cooled), that runs on a power supply operating from 4-50 kV/0.02-1.0 mA at 0.02 increments. The spectrometer is equipped with a 200 l $min^{-1}$ Edwards vacuum pump, allowing for the analysis of lower-atomic-weight elements between sodium (Na) and titanium (Ti). Data acquisition is accomplished with a pulse processor and an analogue-to-digital converter. Elemental composition is identified with digital filter background removal, least squares empirical peak deconvolution, gross peak intensities and net peak intensities above background.

**Trace Element Analysis**

The analysis for mid Zb condition elements Ti-Nb, Pb, Th, the x-ray tube is operated at 30 kV, using a 0.05 mm (medium) Pd primary beam filter in an air path at 100 seconds livetime to generate x-ray intensity $K\alpha_1$-line data for elements titanium (Ti), manganese (Mn), iron (as $Fe_2O_3^T$), cobalt (Co), nickel (Ni), copper, (Cu), zinc, (Zn), gallium (Ga), rubidium (Rb), strontium (Sr), yttrium (Y), zirconium (Zr), niobium (Nb), lead (Pb), and thorium (Th). Not all these elements are reported since their values in many volcanic rocks are very low. Trace element intensities were converted to concentration estimates by employing a linear calibration line ratioed to the Compton scatter established for each element from the analysis of international rock standards certified by the National Institute of Standards and Technology (NIST), the US. Geological Survey (USGS), Canadian Centre for Mineral and Energy Technology, and the Centre de Recherches Pétrographiques et Géochimiques in France (Govindaraju 1994). Line fitting is linear (XML) for all elements. When barium (Ba) is analyzed in the High Zb condition, the Rh tube is operated at 50 kV and up to 1.0 mA, ratioed to the bremsstrahlung region (see Davis 2011; Shackley 2011). Further details concerning the petrological choice of these elements in North Amerian obsidians is available in Shackley (1988, 1995, 2005, 2019b; also Mahood and Stimac 1991; and Hughes and Smith 1993). Nineteen specific pressed powder standards are used for the best fit regression calibration for elements Ti-Nb, Pb, Th, and Ba, and include G-2 (basalt), AGV-2 (andesite), GSP-2 (granodiorite), SY-2 (syenite), BHVO-2 (hawaiite), STM-1 (syenite), QLO-1 (quartz latite), RGM-1 (obsidian), W-2 (diabase), BIR-1 (basalt), SDC-1 (mica schist), TLM-1 (tonalite), SCO-1 (shale), NOD-A-1 and NOD-P-1 (manganese) all US Geological Survey standards, NIST-278 (obsidian), U.S. National Institute of Standards and Technology, BE-N (basalt) from the Centre de Recherches Pétrographiques et Géochimiques in France, and JR-1 and JR-2 (obsidian) from the Geological Survey of Japan (Govindaraju 1994).

**Statistical and Graphical Source Assignment.**

The data from the WinTrace™ software were translated directly into Excel for Windows software for manipulation and on into SPSS ver. 27 and JMP 12.0.1 for statistical analyses. In order to evaluate these quantitative determinations, machine data were compared to measurements of known standards during each run. RGM-1 a USGS obsidian standard is analyzed during each sample run of ≤ 19 for obsidian artifacts to check machine calibration (Table 1).

Source assignments were made by reference to the laboratory database (see Shackley 2005) and the Skinner/Shackley North American Obsidian Database. Further information on the laboratory instrumentation and source data can be found at: http://www.swxrflab.net. Trace element data exhibited in Table 1 and Figure 2 are reported in parts per million (ppm), a quantitative measure by weight.

## SOURCE DISCUSSION

While the obsidian source assemblage was not too diverse, the sources commonly recovered in archaeological contexts, the short descriptions below will have some utility.

**Kane Springs Wash Caldera, Lincoln County, Nevada**

This source, as well as many others in the western Great Basin has received intensive study recently (Johnson and Wagner 2005). About 14 Ma, the Kane Springs caldera collapsed creating an ash flow tuff that quenched rhyolite to obsidian and distributed it over hundreds of square kilometers (Noble 1968; Novak 1984; Novak and Mahood 1986). Similar to the Valles Caldera event in the Jemez Mountains of northern New Mexico, subsequent and final ring eruptions created moat rhyolite domes that quenched to produce obsidian. The earlier and later events that produced obsidian exhibit slightly differing Sr and Ba concentrations, but the sample size in the archaeological assemblage here is too small to discriminate, so no attempt here is made to discriminate the two reported varieties of Kane Springs obsidian (Johnson and Wagner 2005: 36-40). Kane Spring obsidian occurs throughout the Great Basin, although the nodule size at that age are relatively small (marekanites). Its presence in this assemblage seems reasonable (see Figure 1). Artifacts produced from this source were present at sites 5140 and 5354 and comprised 7.9% of the total assemblage (see Table 2 and Figure 1).

**Panaca Summit-Modena Area, Nevada and Utah**

This source, often called simply Modena occurs in a number of alluvial deposits east of Panaca, Lincoln County, Nevada into Utah (Johnson and Haarklau 2005:127). It appears to be eroding out of the Steamboat Mountain Formation near Prohibition Spring (Rowley et al. 2002). This formation dates to 11-13 Ma. Cobble size obsidian occurs at this source, and Modena is one of the more commonly recovered sources in this region, and comprises 65.1% of the total assemblage and was present at all sites (see Table 2 and Figure 1).

**Wild Horse Canyon and Pumice Hole Mine, Beaver County, Utah**

The second most common source recovered from these sites, Wild Horse Canyon obsidian erupted between 800 and 500 ka along the crest of the Mineral Mountains (Lipman et al. 1978). Two chemically distinct compositions are evident, particularly in Zr and can be readily seen in Figure 2 here. Wild Horse Canyon obsidian is present throughout the eastern Great Basin and northern Southwest sites, and was present in Crow Canyon Basketmaker sites (see Shackley 2014, 2017). This source comprised 25.4% of the assemblage and was present in all sites (see Table 2 and Figure 1).

**The Obsidian Cliff Plateau Obsidian Source, Yellowstone Volcanic Field, Northeast Wyoming**

Probably the most well known source of archaeological obsidian in North America, the Obsidian Cliff source has been recovered throughout North America, at least as far east in Mississippian Period contexts in the North American Midwest (Holmes 1879; Davis et al. 1995). Part of the Quaternary Canyon Rhyolite formation, it is directly related to the Yellowstone Caldera event and is one of the largest single blocks of obsidian on earth (Boyd 1961; Christiansen and Blank 1972; Iddings 1888). The event occurred based on K-Ar dating at 183±0.003 ka and the obsidian covers an area of approximately 14.5 $km^2$ with an exposed thickness of 30 m (Schmitt 1995 in Davis et al. 1995). The sheer size of quenching to glass of this structure was due to eruption into the continental glacier that at that time was over 2 km thick. The ice facilitated quenching the rhyolite at a very rapid rate. The one piece of debitage here from site 4098 comprises only 1.6% of the assemblage. It is likely that that piece of debitage is the result of production or rejuvenation of a biface.

**Procurement Range/Social Networking**

I found it intriguing that there were no artifacts produced from Jemez Mountain or Mount Taylor obsidian sources of northern New Mexico. These sources are common in Archaic through PIII sites in the region, particularly in the later periods. It could be sampling error, but the assemblage indicates a relatively local procurement range or social network focused to the west and north.

## REFERENCES CITED


Beck, Charlotte and George T. Jones, 2011, The Role of Mobility and Exchange in the Conveyance of Toolstone During the Great Basin Paleoarchaic. In R. E. Hughes (Ed.) Perspectives on Prehistoric Trade and Exchange in California and the Great Basin, pp. 55-82. The University of Utah Press, Salt Lake City, Utah.

Boyd, F.R. 1961, Welded tuffs and flows in the rhyolite plateau of Yellowstone Park, Wyoming. *Geological Society of America Bulletin* 72:387-426.

Christiansen, R.L. and H.R. Blank, 1972, *Volcanic stratigraphy of the Quaternary rhyolite plateau in Yellowstone National Park*. U.S. Geological Survey Professional Paper 729-B.

Davis, L.B., S.A. Aaberg, J.G. Schmitt, and A. M. Johnson, 1995, *The Obsidian Cliff Plateau Prehistoric Lithic Source, Yellowstone National Park, Wyoming*. National Park Service, Division of Cultural Resources Selection Series 6, Denver, Colorado.

Davis, M.K., T.L. Jackson, M.S. Shackley, T. Teague, and J. Hampel, 2011, Factors Affecting the Energy-Dispersive X-Ray Fluorescence (EDXRF) Analysis of Archaeological Obsidian. In M.S. Shackley (Ed.) *X-Ray Fluorescence Spectrometry (XRF) in Geoarchaeology*, pp. 45-64. Springer, New York.

Govindaraju, K., 1994 , 1994 Compilation of Working Values and Sample Description for 383 Geostandards. *Geostandards Newsletter* 18 (special issue).

Hampel, Joachim H., 1984, Technical Considerations in X-ray Fluorescence Analysis of Obsidian. In R.E. Hughes (Ed.) *Obsidian Studies in the Great Basin*, pp. 21-25. Contributions of the University of California Archaeological Research Facility 45. Berkeley.

Haarklau, L, L. Johnson, and D.L. Wagner, 2005, *Fingerprints in the Great Basin: The Nellis Air Force Base Regional Obsidian Sourcing Study*. U.S. Army Corps of Engineers, Fort Worth District.

Hildreth, W., 1981, Gradients in Silicic Magma Chambers: Implications for Lithospheric Magmatism. *Journal of Geophysical Research* 86:10153-10192.

Holmes, W.H. 1879, Notes on an extensive deposit of obsidian in the Yellowstone National Park. *American Naturalist* 13:247-250.

Hughes, Richard E., and Robert L. Smith, 1993, Archaeology, Geology, and Geochemistry in Obsidian Provenance Studies. In J.K. Stein and A.R. Linse (Eds.) *Scale on Archaeological and Geoscientific Perspectives*, pp. 79-91. Geological Society of America Special Paper 283.

Iddings, J.P. 1888, *Obsidian Cliff, Yellowstone National Park*. Seventh Annual Report of the U.S. Geological Survey, Washington, DC.

Johnson, L., and D.L. Wagner, 2005, Obsidian source characterization study. In Haarklau, Johnson, and Wagner (Eds.), *Fingerprints in the Great Basin: The Nellis Air Force Base Regional Obsidian Sourcing Study*. U.S. Army Corps of Engineers, Fort Worth District, pp. 25-50.

Lipman, P.W., P.D. Rowley, H.H. Mehnert, S.H. Evans Jr., W.P. Nash, and F.H. Brown, 1978, Pleistocene rhyolite of the Mineral Mountains, Utah-Geothermal and Archaeological Significance. *Journal of Research, U.S. Geological Survey* 6:133-147.

Mahood, Gail A., and James A. Stimac, 1990, Trace-Element Partitioning in Pantellerites and Trachytes. *Geochemica et Cosmochimica Acta* 54:2257-2276.

McCarthy, J.J., and F.H. Schamber, 1981, Least-Squares Fit with Digital Filter: A Status Report. In K.F.J. Heinrich, D.E. Newbury, R.L. Myklebust, and C.E. Fiori (Eds.) *Energy Dispersive X-ray Spectrometry*, pp. 273-296. National Bureau of Standards Special Publication 604, Washington, D.C.

Noble, D.C. 1968, Kane Springs Wash volcanic center, Lincoln County, Nevada. In E.B. Eckel (Ed.), *Nevada Test Site*, Geological Society of America Memoir 110, pp. 109-116.

Novak, S.W. 1984, Eruptive history of the rhyolitic Kane Springs Wash volcanic center, Nevada. *Journal of Geophysical Research* 89(B10):8603-8615.

Novak, S.W., and G.A. Mahood, 1986, Rise and fall of a basalt-trachyte-rhyolite magma system at the Kane Spring Wash caldera, Nevada. *Contributions to Mineralogy and Petrology* 94:352-373.

Rowley, P.D., F.W. Lytle, M.B. Lytle, and K.R. Stever, 2002, Geology of the Modena Obsidian Source, Lincoln County, Nevada. Report on file at BLM, Ely Field Office.

Schamber, F.H., 1977, A Modification of the Linear Least-Squares Fitting Method which Provides Continuum Suppression. In T.G. Dzubay (Ed.) *X-ray Fluorescence Analysis of Environmental Samples*, pp. 241-257. Ann Arbor Science Publishers.

Scheiber, Laura L., and Judson B. Finley, 2011, Obsidian Source Use in the Greater Yellowstone Area, Wyoming Basin, and Central Rocky Mountains. *American Antiquity* 76:372-394

Shackley, M.S., 1988, Sources of Archaeological Obsidian in the Southwest: An Archaeological, Petrological, and Geochemical Study. *American Antiquity* 53:752-772.

Shackley, M. S.,1995, Sources of Archaeological Obsidian in the Greater American Southwest: An Update and Quantitative Analysis. *American Antiquity* 60(3):531-551.

Shackley, M.S., 2005, *Obsidian: Geology and Archaeology in the North American Southwest*. University of Arizona Press, Tucson.

Shackley, M.S., 2011, An Introduction to X-Ray Fluorescence (XRF) Analysis in Archaeology. In *X-Ray Fluorescence Spectrometry (XRF) in Geoarchaeology*, M.S. Shackley (Ed.), pp. 7-44. Springer, New York.

Shackley, M.S., 2014, Source Provenance of Obsidian Artifacts from Various Sites in the Goodman Point Project, Montezuma County, Southwest Colorado. Report prepared for Crow Canyon Archaeological Center, Cortez, Colorado.

Shackley, M.S., 2017, An Energy-Dispersive X-Ray Fluorescence Analysis of Obsidian Artifacts from Four Sites in Southwestern Colorado. Report prepared for Crow Canyon Archaeological Center, Cortez, Colorado.

Table 1. Elemental concentrations and source assignments for the archaeological samples and USGS RGM-1 rhyolite standard. All measurement in parts per million (ppm).

| Sample | Site | Ti | Mn | Fe | Rb | Sr | Y | Zr | Nb | Ba | Ce | Pb | Th | Source |
|---|---|---|---|---|---|---|---|---|---|---|---|---|---|---|
| 1 | 42WS3836 | 1027 | 283 | 9447 | 196 | 85 | 27 | 124 | 18 | 541 | 46 | 27 | 40 | Modena, UT |
| 2 | 42WS3836 | 1195 | 372 | 9448 | 216 | 46 | 28 | 119 | 24 | 227 | 8 | 32 | 18 | Wild Horse Canyon, UT |
| 3 | 42WS3836 | 1233 | 322 | 10174 | 214 | 89 | 30 | 122 | 23 | 564 | 67 | 28 | 31 | Modena, UT |
| 4 | 42WS3836 | 1153 | 323 | 10006 | 209 | 90 | 21 | 130 | 18 | 532 | 50 | 28 | 35 | Modena, UT |
| 5 | 42WS3836 | 1275 | 379 | 9661 | 217 | 43 | 21 | 124 | 25 | 189 | 35 | 32 | 19 | Wild Horse Canyon, UT |
| 6 | 42WS3836 | 1253 | 382 | 9498 | 218 | 47 | 25 | 128 | 26 | 206 | 47 | 34 | 28 | Wild Horse Canyon, UT |
| 7 | 42WS3836 | 1374 | 388 | 10680 | 200 | 70 | 28 | 141 | 27 | 364 | 0 | 30 | 21 | Modena, UT |
| 8 | 42WS3836 | 1072 | 375 | 9382 | 209 | 50 | 23 | 121 | 22 | 224 | 38 | 28 | 20 | Wild Horse Canyon, UT |
| 9 | 42WS3836 | 1186 | 352 | 10456 | 203 | 87 | 30 | 121 | 20 | 572 | 34 | 30 | 34 | Modena, UT |
| 10 | 42WS3836 | 1225 | 344 | 10249 | 211 | 87 | 31 | 134 | 26 | 614 | 37 | 32 | 31 | Modena, UT |
| 11 | 42WS3836 | 1156 | 345 | 9045 | 195 | 45 | 24 | 114 | 26 | 174 | 51 | 28 | 26 | Wild Horse Canyon, UT |
| 12 | 42WS3836 | 1258 | 323 | 10259 | 216 | 85 | 28 | 137 | 22 | 598 | 41 | 29 | 26 | Modena, UT |
| 13 | 42WS3836 | 1212 | 388 | 9400 | 208 | 47 | 26 | 119 | 28 | 227 | 35 | 37 | 32 | Wild Horse Canyon, UT |
| 14 | 42WS3836 | 1198 | 403 | 9398 | 205 | 42 | 23 | 121 | 29 | 207 | 15 | 26 | 31 | Wild Horse Canyon, UT |
| 15 | 42WS3836 | 1125 | 325 | 10075 | 210 | 88 | 35 | 126 | 20 | 574 | 43 | 28 | 37 | Modena, UT |
| 16 | 42WS3836 | 1090 | 335 | 9805 | 210 | 89 | 34 | 132 | 20 | 581 | 43 | 27 | 31 | Modena, UT |
| 17 | 42WS3836 | 1214 | 340 | 9637 | 199 | 48 | 29 | 117 | 25 | 203 | 50 | 28 | 24 | Wild Horse Canyon, UT |
| 18 | 42WS4098 | 1435 | 389 | 11475 | 246 | 98 | 28 | 120 | 14 | 414 | 5 | 37 | 25 | Modena, UT |
| 19 | 42WS4098 | 1161 | 260 | 10995 | 184 | 22 | 43 | 160 | 39 | 49 | 70 | 20 | 30 | Wild Horse Canyon, UT* |
| 20 | 42WS409 | 126 | 351 | 1059 | 226 | 94 | 27 | 135 | 20 | 555 | 33 | 27 | 34 | Modena, UT |

| | | | | | | | | | | | | | | |
|---|---|---|---|---|---|---|---|---|---|---|---|---|---|---|
| | 8 | 7 | | 0 | | | | | | | | | | |
| 21 | 42WS4098 | 1084 | 374 | 9331 | 204 | 50 | 24 | 117 | 20 | 218 | 49 | 30 | 29 | Wild Horse Canyon, UT |
| 22 | 42WS4098 | 1216 | 313 | 10409 | 222 | 86 | 28 | 130 | 23 | 575 | 44 | 34 | 34 | Modena, UT |
| 23 | 42WS4098 | 899 | 320 | 13069 | 259 | 12 | 63 | 195 | 46 | 0 | 27 | 40 | 38 | Obsidian Cliff, WY |
| 24 | 42WS4098 | 1219 | 342 | 10252 | 209 | 79 | 29 | 126 | 20 | 559 | 58 | 33 | 43 | Modena, UT |
| 25 | 42WS4098 | 1344 | 330 | 10812 | 218 | 90 | 34 | 125 | 19 | 464 | 43 | 33 | 28 | Modena, UT |
| 26 | 42WS5133 | 1079 | 323 | 9597 | 204 | 84 | 26 | 129 | 13 | 602 | 86 | 26 | 33 | Modena, UT |
| 27 | 42WS5133 | 1138 | 300 | 9183 | 194 | 80 | 32 | 125 | 20 | 649 | 109 | 25 | 29 | Modena, UT |
| 28 | 42WS5133 | 1338 | 396 | 10582 | 204 | 51 | 26 | 113 | 20 | 213 | 54 | 35 | 33 | Wild Horse Canyon, UT |
| 29 | 42WS5133 | 1239 | 427 | 9878 | 211 | 53 | 25 | 115 | 24 | 217 | 0 | 23 | 22 | Wild Horse Canyon, UT |
| 30 | 42WS5133 | 1242 | 354 | 10602 | 222 | 83 | 34 | 132 | 23 | 531 | 30 | 32 | 32 | Modena, UT |
| 31 | 42WS5133 | 1126 | 331 | 9777 | 206 | 87 | 32 | 134 | 25 | 650 | 86 | 28 | 41 | Modena, UT |
| 32 | 42WS5140 | 1160 | 348 | 10268 | 200 | 86 | 34 | 131 | 22 | 565 | 38 | 28 | 24 | Modena, UT |
| 33 | 42WS5140 | 1034 | 310 | 9459 | 200 | 83 | 30 | 125 | 21 | 601 | 59 | 26 | 32 | Kane Springs, NV |
| 34 | 42WS5140 | 1109 | 271 | 11278 | 204 | 49 | 32 | 157 | 27 | 306 | 52 | 22 | 34 | Wild Horse Canyon, UT |
| 35 | 42WS5140 | 1143 | 354 | 10173 | 219 | 86 | 31 | 133 | 28 | 591 | 64 | 34 | 35 | Modena, UT |
| 36 | 42WS5140 | 1177 | 312 | 10272 | 216 | 85 | 33 | 128 | 22 | 615 | 34 | 26 | 20 | Modena, UT |
| Sample | Site | Ti | Mn | Fe | Rb | Sr | Y | Zr | Nb | Ba | Ce | Pb | Th | Source |
| 37 | 42WS5140 | 1107 | 328 | 10147 | 217 | 91 | 35 | 136 | 21 | 568 | 29 | 29 | 26 | Modena, UT |
| 38 | 42WS5140 | 1220 | 338 | 9540 | 175 | 69 | 24 | 133 | 23 | 355 | 37 | 26 | 19 | Modena, UT |
| 39 | 42WS5140 | 1307 | 437 | 10409 | 218 | 45 | 27 | 112 | 27 | 185 | 24 | 35 | 29 | Wild Horse Canyon, UT |
| 40 | 42WS5140 | 1134 | 312 | 9949 | 209 | 89 | 33 | 129 | 22 | 570 | 47 | 26 | 29 | Modena, UT |
| 41 | 42WS5140 | 1248 | 371 | 10676 | 222 | 88 | 32 | 128 | 18 | 593 | 38 | 32 | 36 | Modena, UT |

| | | | | | | | | | | | | | |
|---|---|---|---|---|---|---|---|---|---|---|---|---|---|
| 42 | 42WS5140 | 1144 | 347 | 10074 | 215 | 87 | 37 | 129 | 17 | 588 | 58 | 28 | 36 | Modena, UT |
| 43 | 42WS5140 | 1236 | 341 | 10415 | 220 | 92 | 26 | 125 | 24 | 584 | 43 | 29 | 37 | Modena, UT |
| 44 | 42WS5140 | 1107 | 310 | 9401 | 195 | 83 | 26 | 138 | 21 | 593 | 67 | 27 | 20 | Modena, UT |
| 45 | 42WS5140 | 1085 | 314 | 9499 | 195 | 83 | 27 | 119 | 24 | 577 | 68 | 26 | 27 | Modena, UT |
| 46 | 42WS5140 | 1072 | 322 | 9503 | 203 | 86 | 34 | 118 | 22 | 602 | 49 | 29 | 27 | Modena, UT |
| 47 | 42WS5140 | 1167 | 332 | 9865 | 205 | 88 | 26 | 127 | 21 | 562 | 53 | 25 | 37 | Kane Springs, NV |
| 48 | 42WS5140 | 1150 | 309 | 12032 | 216 | 50 | 41 | 156 | 23 | 329 | 34 | 27 | 38 | Wild Horse Canyon, UT |
| 49 | 42WS5140 | 1240 | 332 | 10177 | 214 | 87 | 33 | 134 | 18 | 609 | 52 | 27 | 41 | Modena, UT |
| 50 | 42WS5140 | 1138 | 309 | 9878 | 212 | 88 | 28 | 127 | 17 | 614 | 34 | 32 | 30 | Modena, UT |
| 51 | 42WS5140 | 1146 | 355 | 10553 | 218 | 91 | 29 | 127 | 18 | 516 | 29 | 27 | 38 | Modena, UT |
| 52 | 42WS5140 | 1206 | 311 | 9508 | 200 | 86 | 29 | 120 | 20 | 566 | 74 | 27 | 39 | Modena, UT |
| 53 | 42WS5354 | 1333 | 354 | 9075 | 192 | 40 | 22 | 114 | 21 | 183 | 16 | 29 | 13 | Wild Horse Canyon, UT |
| 54 | 42WS5354 | 1082 | 315 | 9530 | 202 | 84 | 36 | 122 | 27 | 604 | 95 | 29 | 34 | Modena, UT |
| 55 | 42WS5354 | 1226 | 334 | 10025 | 209 | 89 | 28 | 123 | 19 | 608 | 48 | 34 | 33 | Modena, UT |
| 56 | 42WS5354 | 1120 | 300 | 11764 | 205 | 50 | 40 | 158 | 25 | 332 | 49 | 22 | 35 | Kane Springs, NV |
| 57 | 42WS5354 | 1054 | 313 | 11558 | 203 | 46 | 36 | 156 | 31 | 313 | 43 | 22 | 28 | Kane Springs, NV |
| 58 | 42WS5354 | 1111 | 279 | 11535 | 205 | 51 | 37 | 161 | 24 | 345 | 62 | 23 | 37 | Kane Springs, NV |
| 59 | 42WS5354 | 1276 | 396 | 10449 | 211 | 86 | 31 | 128 | 26 | 603 | 75 | 29 | 34 | Modena, UT |
| 60 | 42WS5354 | 1032 | 322 | 9376 | 198 | 82 | 29 | 132 | 22 | 621 | 97 | 27 | 35 | Modena, UT |
| 61 | 42WS5354 | 753 | 153 | 5672 | 0 | 21 | 4 | 16 | 4 | 36 | 16 | -1 | 4 | not obsidian |
| 62 | 42WS5354 | 1142 | 324 | 9400 | 199 | 80 | 28 | 135 | 20 | 620 | 111 | 23 | 30 | Modena, UT |
| 63 | 42WS5354 | 776 | 158 | 5986 | 5 | 27 | 6 | 27 | 4 | 20 | 20 | 2 | 4 | not obsidian |

| | | | | | | | | | | | | | | |
|---|---|---|---|---|---|---|---|---|---|---|---|---|---|---|
| 64 | 42WS5354 | 765 | 150 | 5861 | 0 | 18 | 5 | 17 | 3 | 30 | 15 | 2 | 6 | not obsidian |
| 65 | 42WS5354 | 1194 | 301 | 9548 | 204 | 83 | 30 | 125 | 23 | 638 | 44 | 27 | 25 | Modena, UT |
| 66 | 42WS5354 | 1288 | 365 | 9843 | 200 | 68 | 28 | 148 | 32 | 454 | 59 | 31 | 29 | Modena, UT |
| RGM1-S4 | | 1480 | 305 | 13077 | 149 | 105 | 24 | 217 | 7 | 813 | 45 | 23 | 26 | standard |
| RGM1-S4 | | 1568 | 294 | 13116 | 153 | 105 | 25 | 221 | 11 | 822 | 18 | 16 | 16 | standard |
| RGM1-S4 | | 1596 | 294 | 13323 | 150 | 107 | 26 | 219 | 12 | 826 | 49 | 21 | 15 | standard |

Table 2. Crosstabulation of source by site. Non-obsidian samples not included (see Table 1).

| | | | Source | | | | |
|---|---|---|---|---|---|---|---|
| | | | Kane Springs, NV | Modena, UT | Obsidian Cliff, WY | Wild Horse Canyon, UT | Total |
| Site | 42WS3836 | Count | 0 | 9 | 0 | 8 | 17 |
| | | % within Site | 0.0% | 52.9% | 0.0% | 47.1% | 100.0% |
| | | % within Source | 0.0% | 22.0% | 0.0% | 50.0% | 27.0% |
| | | % of Total | 0.0% | 14.3% | 0.0% | 12.7% | 27.0% |
| | 42WS4098 | Count | 0 | 5 | 1 | 2 | 8 |
| | | % within Site | 0.0% | 62.5% | 12.5% | 25.0% | 100.0% |
| | | % within Source | 0.0% | 12.2% | 100.0% | 12.5% | 12.7% |
| | | % of Total | 0.0% | 7.9% | 1.6% | 3.2% | 12.7% |
| | 42WS5133 | Count | 0 | 4 | 0 | 2 | 6 |
| | | % within Site | 0.0% | 66.7% | 0.0% | 33.3% | 100.0% |
| | | % within Source | 0.0% | 9.8% | 0.0% | 12.5% | 9.5% |
| | | % of Total | 0.0% | 6.3% | 0.0% | 3.2% | 9.5% |
| | 42WS5140 | Count | 2 | 16 | 0 | 3 | 21 |
| | | % within Site | 9.5% | 76.2% | 0.0% | 14.3% | 100.0% |
| | | % within Source | 40.0% | 39.0% | 0.0% | 18.8% | 33.3% |
| | | % of Total | 3.2% | 25.4% | 0.0% | 4.8% | 33.3% |
| | 42WS5354 | Count | 3 | 7 | 0 | 1 | 11 |
| | | % within Site | 27.3% | 63.6% | 0.0% | 9.1% | 100.0% |
| | | % within Source | 60.0% | 17.1% | 0.0% | 6.3% | 17.5% |
| | | % of Total | 4.8% | 11.1% | 0.0% | 1.6% | 17.5% |
| Total | | Count | 5 | 41 | 1 | 16 | 63 |
| | | % within Site | 7.9% | 65.1% | 1.6% | 25.4% | 100.0% |
| | | % within Source | 100.0% | 100.0% | 100.0% | 100.0% | 100.0% |
| | | % of Total | 7.9% | 65.1% | 1.6% | 25.4% | 100.0% |

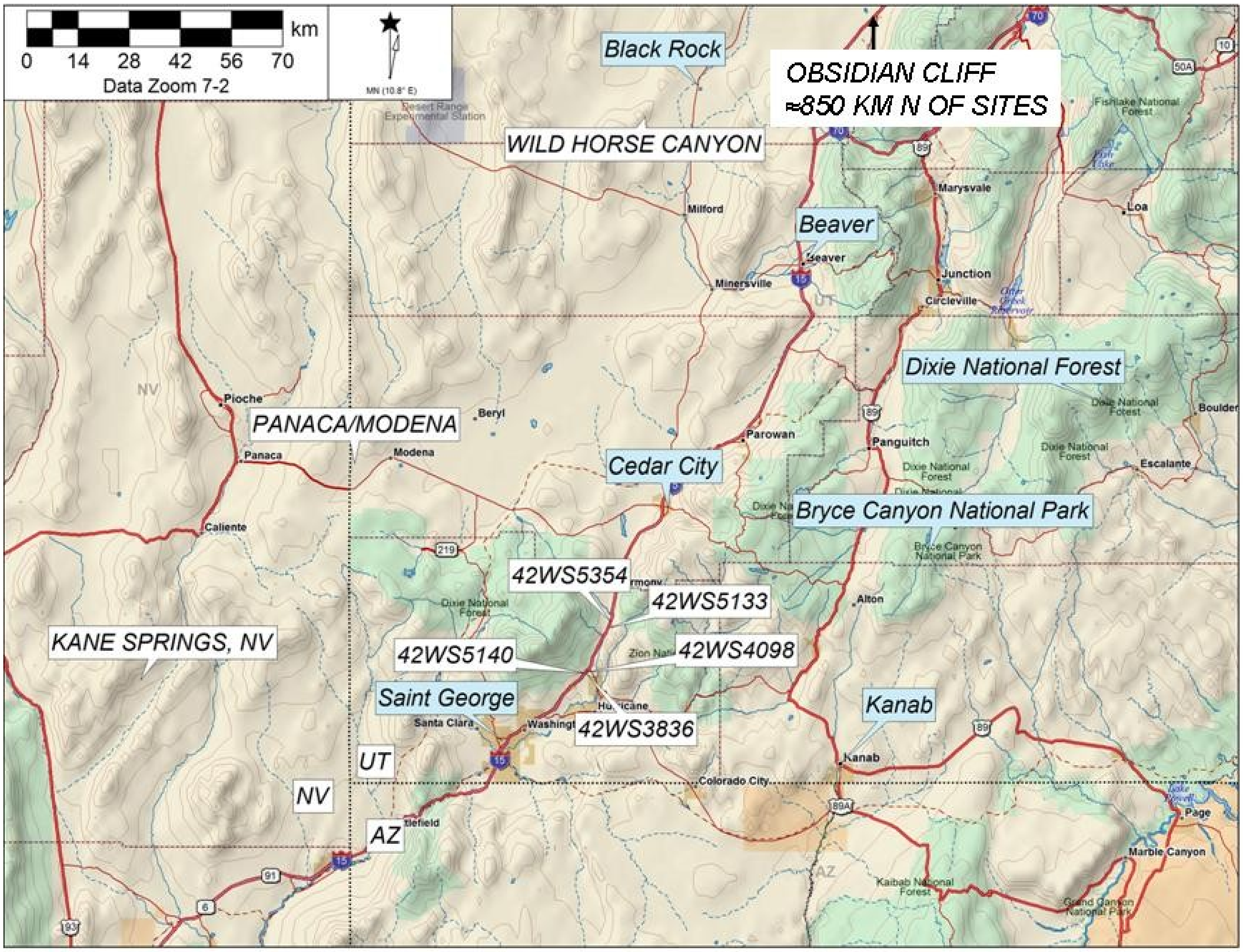


Figure 1. Location of identified obsidian sources (capitals) in southwest Utah and southeast Nevada.

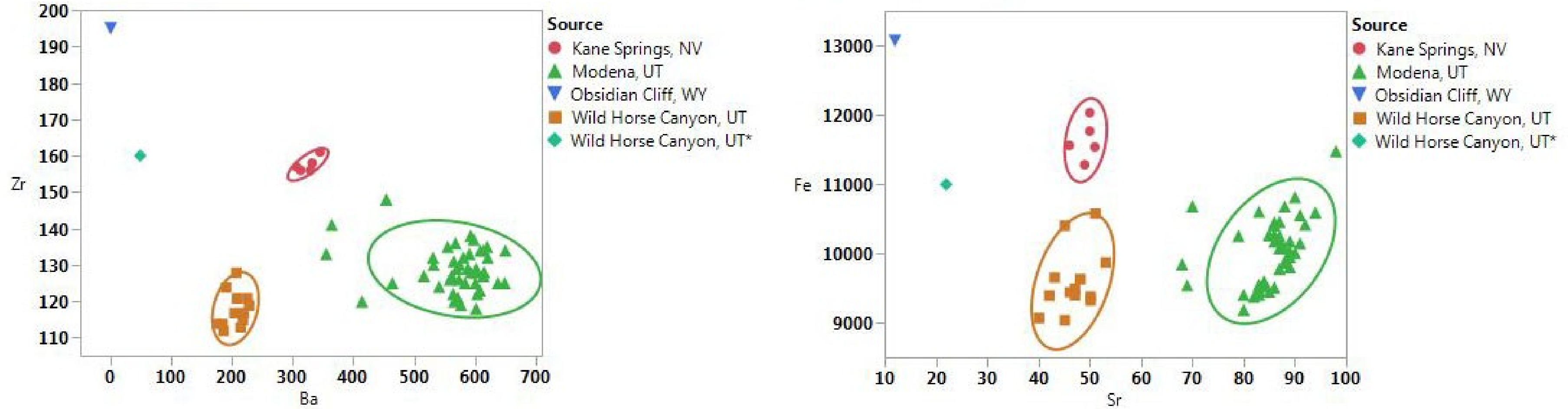


Figure 2. Ba/Zr (left) and Sr/Fe (right) bivariate plots of all samples. Confidence ellipses at 90%. Asterisked Wild Horse Canyon was a very small sample that otherwise fit the source composition, but is probably too small to confidently assign to source (see Davis et al. 2011).